

Article

Rhodium Nanoparticles Incorporated Mesoporous Silica as an Active Catalyst for Cyclohexene Hydrogenation under Ambient Conditions

Mohamed S. Hamdy ¹, Abdullah M. Alhanash ¹, Mhamed Benaissa ², Ali Alsalmeh ³, Fahad A. Alharthi ³ and Nabil Al-Zaqri ^{3,*}

¹ Catalysis Research Group (CRG), Department of Chemistry, College of Science, King Khalid University, P.O. Box 9004, Abha 61413, Saudi Arabia; m.s.hamdy@gmail.com (M.S.H.); alhnsh@kku.edu.sa (A.M.A.)

² Chemical Engineering Department, College of Engineering, University of Hail, P.O. Box 2440, Hail 81451, Saudi Arabia; mhamedbenaissa03@gmail.com

³ Department of Chemistry, College of Science, King Saud University, P.O. Box 2455, Riyadh 11451, Saudi Arabia; aalsalme@ksu.edu.sa (A.A.); fharthi@ksu.edu.sa (F.A.A.)

* Correspondence: nalzaqri@ksu.edu.sa; Tel.: +966-5021-3-2010

Received: 27 July 2020; Accepted: 10 August 2020; Published: 12 August 2020



Abstract: Rhodium (Rh) nanoparticles were embedded in the mesopores of TUD-1 siliceous material and denoted as Rh-TUD-1. Five samples of Rh-TUD-1 were prepared with different loadings of Rh that ranged from 0.1 to 2 wt% using the sol-gel technique. The prepared samples were characterized by means of several chemical and physical techniques. The obtained characterization results show the formation of highly distributed Rh⁰ nanoparticles with an average size ranging from 3 to 5 nm throughout the three-dimensional silica matrix of TUD-1. The catalytic activity of the prepared catalysts was evaluated in the solvent-free hydrogenation of cyclohexene to cyclohexane at room temperature using 1atm of hydrogen gas. The obtained catalytic results confirm the high activity of Rh-TUD-1, in which a turn over frequency (TOF) ranging from 4.94 to 0.54 s⁻¹ was obtained. Moreover, the change in reaction temperature during the reaction was monitored, and it showed an obvious increase in the reaction temperature as an indication of the spontaneous and exothermic nature of the reactions. Other optimization parameters, such as the substrate/catalyst ratio, and performing the reaction under non-ambient conditions (temperature = 60 °C and hydrogen pressure = 5 atm) were also investigated. Rh-TUD-1 exhibited a high stability in a consecutive reaction of five runs under either ambient or non-ambient conditions.

Keywords: Rh-TUD-1; nanoparticles; hydrogenation; cyclohexene; stability; activity

1. Introduction

The catalytic hydrogenation of double bonds in alkenes is an essential process for both fundamental and applied studies on hydrocarbon conversion chemistry and other chemical industries [1–3]. The hydrogenation reactions of cycloalkenes have been widely used as model reactions for fundamental investigations of catalysis and examining the catalytic activity of newly developed heterogeneous catalysts [3,4]. Cyclohexane, the product of cyclohexene hydrogenation, is a critical intermediate in the nylon industry [5,6]. Therefore, the hydrogenation of cyclohexene is well-studied in the liquid phase at ambient conditions using homogeneous catalysts such as Wilkinson-type catalysts and other transition metal complexes [7,8]. However, due to environmental and economic concerns, heterogeneous catalysis is of great interest in industrial applications. Therefore, the hydrogenation of cycloalkenes has been widely studied using supported noble metals and metal oxides [9–11].

Catalytic hydrogenation is a bimolecular reaction in which hydrogen and unsaturated alkenes are expected to be adsorbed onto the catalytic surface. Therefore, conducting the hydrogenation of cycloalkenes in a heterogeneous catalytic system makes it susceptible to several variables, some of which are related to the catalytic materials, such as the metal type and form, the metal loading, and the type of support. Noble metals have shown a high activity in heterogeneous hydrogenation reactions. However, for improved activity as well as economic reasons, structurally defined and highly dispersed metallic nanoparticles on proper support with a high surface is an attractive alternative to bulk metal catalysts.

The use of supported noble metal nanoparticles in the hydrogenation of cyclohexene attracts interest, however it has not been deeply investigated. Few bio-based supports were used to accommodate the noble metal nanoparticles. Oliveira et al. [12] used cellulose acetate membranes to support palladium and rhodium nanoparticles, and the prepared catalysts exhibited a high activity in cyclohexene hydrogenation. Moreover, Ghadamgahi et al. [13] reported recently the use of palladium nanoparticles supported on wool in the hydrogenation of cyclohexene under elevated temperature and pressure. On the other hand, mesoporous silica materials were applied to support the different noble metal nanoparticles because of their high stability under high pressure and temperature, in addition to their high surface area and wide pore volume. Feil et al. [14] reported the deposition of palladium nanoparticles onto SBA-15 mesoporous material, and the prepared catalyst was used to catalyze the reduction of cyclohexene at an elevated temperature and pressure—i.e., a 75 °C and 4 bar hydrogen gas pressure. Moreover, in a third study Patel et al. [15] reported the use of MCM-41 mesoporous siliceous material to support palladium nanoparticles together with monolacunary silicotungstate; the prepared catalyst exhibited a high activity in the hydrogenation of cyclohexene at 80 °C and 10 bar of hydrogen gas pressure. Rhodium-based complexes were applied successfully as very active homogeneous catalysts for cyclohexene hydrogenation [16]. However, limited research was reported to design a heterogeneous catalyst based on Rh nanoparticles as active sites because of the instability of Rh nanoparticles, as reported by Philippot et al. [17]. Several trials were reported to overcome the instability of Rh nanoparticles in hydrogenation reactions, such as the use of microwave in the synthesis of Rh nanoparticles [18], and the core-shell design with another noble metal such as gold [19]. Therefore, the synthesis of an Rh-based heterogeneous catalyst with a high activity and high stability represents one of the challenges in the catalysis world.

The team of the current research has established an extended investigation into the solvent-free liquid-phase hydrogenation of cycloalkenes using metals nanoparticles supported in the three-dimensional mesoporous silica TUD-1 at ambient conditions [20–22]. Pd-TUD-1 exhibited a superior activity in the selective hydrogenation of 1,5-cyclooctadiene under solvent-free conditions [21,22]. TUD-1 is a siliceous mesoporous material which was patented in 2001 by Shan et al. [23]. TUD-1 features its easy synthetic procedure where no surfactant is needed, which makes it a cost-effective support. Moreover, TUD-1 possesses a unique siliceous structure different from the conventional mesoporous materials such as MCM-41 and SBA-15 due to its open and 3D pore system. TUD-1 was used as a support for different metal ions or oxide particles, such as Au [24], Mo [25], Cr [26], V [27], etc. All the mentioned catalysts were prepared with different metal loadings using a one-step synthesis procedure without the use of any surfactant or co-polymer. The prepared catalysts exhibited a high activity in different catalytic reactions; for example, Au-TUD-1 exhibited a high activity in the aerobic oxidation of cyclohexene [24], Mo-TUD-1 exhibited a high activity in the epoxidation of cyclohexene [25], Cr-TUD-1 exhibited a superior photocatalytic activity in the elimination of short-chain hydrocarbons, and V-TUD-1 was used to investigate the photocatalytic oxidation of cyclohexene by time-resolved ATR-FTIR spectroscopy [27].

In a recent study [20], the current research team reported the preliminary results of the incorporation of rhodium nanoparticles ($\approx 3\text{--}5$ nm) into the 3D mesoporous TUD-1, which exhibited a high activity in the liquid phase conversion of cyclohexene to cyclohexane at room temperature, 1atm H₂ pressure, and under solvent-free conditions. Rhodium nanoparticles exhibited a high stability and reusability and negligible leaching. Due to the critical role of Rh nanoparticles in these hydrogenation reactions

and these promising results of Rh nanoparticles at such conditions, further investigation on the effect of Rh content on the overall activity of this reaction is encouraged. Therefore, in the present work, five samples of Rh were prepared with different loadings of Rh from 0.1 to 2 wt% using the sol-gel technique, as reported previously [26,28]. The reduced Rh nanoparticles incorporating TUD-1 were characterized by means of powder X-ray diffraction (XRD), inductive coupled plasma (ICP) elemental analysis, N₂ physisorption, X-ray photoelectron spectroscopy (XPS), and high-resolution transmission electron microscopy (HR-TEM). Moreover, the catalytic activity of the prepared catalysts were evaluated in the solvent-free hydrogenation of cyclohexene to cyclohexane under ambient and non-ambient conditions.

2. Results

2.1. The Composition of the Prepared Catalysts

The amount of Rh in the prepared Rh-TUD-1 samples was calculated using the ICP technique, and the obtained results are compared with the amount of Rh in the synthesis mixture in Figure 1a and in Table 1. The obtained results showed that the Rh content % in the final product is very close to the amount which was added in the synthesis mixture. In other words, all the Rh which was added during the synthesis was obtained in the final solid product. Hence, this result indicates the high efficiency and good predictability of the synthesis procedure. Similar results were reported earlier in [25,28].

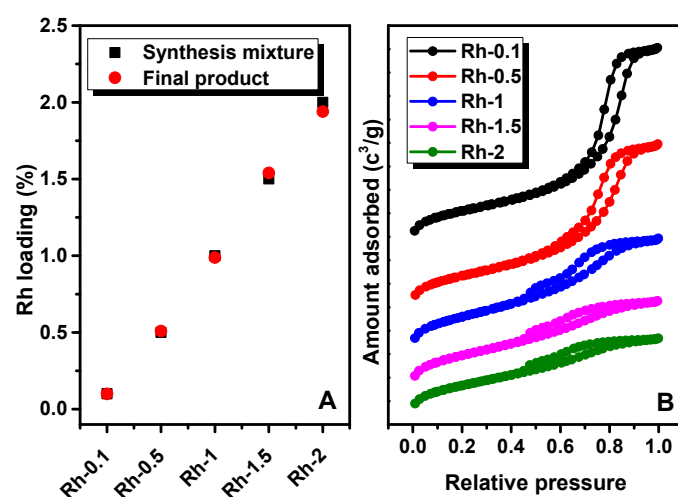


Figure 1. (A) Comparison between the Rh% loading in the synthesis gel and in the obtained final solid product. (B) N₂ sorption isotherms for the prepared Rh-TUD-1 samples.

Table 1. The Rh% in the prepared Rh-TUD-1 samples, as obtained from elemental analysis, compared with that in the synthesis gel. Moreover, the texture properties of the prepared Rh-TUD-1, as obtained from the N₂ sorption measurement.

Samples	Rh Loading (wt %)		Texture Properties		
	Synthesis Gel	Final Product	Surface Area m ² /g	Pore Volume cm ³ /g	Pore Size nm
TUD-1	0	0	605.6	0.64	4.2
Rh-0.1	0.1	0.099	614.2	1.33	7.3
Rh-0.5	0.5	0.509	634.3	1.14	6.5
Rh-1	1	0.988	685.9	0.80	5.9
Rh-1.5	1.5	1.44	653.3	0.63	5.3
Rh-2	2	1.94	595.8	0.56	4.8

The mesoporous character of the prepared samples was studied using the N₂ sorption technique. The N₂ sorption isotherms are present in Figure 1b. All the prepared samples exhibited type IV isotherm,

which, according to the IUPAC classification [29], is characteristic of the presence of mesoporous solid material. Moreover, the hysteresis loops in the isotherms changed from type H1 to type H3 with the increasing Rh loading. This can be explained by the partial blocking of the mesopore by Rh nanoparticles, which increased with increasing the Rh content. Therefore, the pore's nature changed from uniform and cylindrical with no intraconnectivity (H1) to non-uniform pores (H3). The pore volume and pore size were found to be decreased (Table 1) with increasing the Rh content due to the increase in the Rh nanoparticles inside the pores of TUD-1 (partial blocking). However, there is no simple trend in the case of surface area; the surface area increased in the Rh-1.5 sample and decreased in the case of Rh-2, which was most likely due to the total blocking of some mesopores by Rh nanoparticles. Similar trends were also reported for Fe-TUD-1 [30] and Mo-TUD-1 [25].

The degree of crystallinity of the prepared samples was investigated using the XRD technique before and after the hydrogenation step of the reduction. The obtained XRD patterns are presented in Figure 2. All the patterns show a broad band around 23° – 25° 2θ , which is characteristic of the amorphous phase of silica [26]. In Figure 2a, in the patterns before reduction, the peaks of the β - Rh_2O_3 phase were clearly visible at 24.4° , 32.9° , 34.98° , 44.0° , 48.77° , 53.3° , 57.17° , 61.57° , and 67.54° 2θ [31], which match the locations of the rhodium oxide phase in Joint Committee on Powder Diffraction Standards (JCPDS) card number 76-0148. The presence of these peaks confirms the formation of rhodium oxide nanoparticles in the as-synthesized Rh-TUD-1 samples. Moreover, after the reduction, all the patterns (except that of Rh-1) show peaks at 41.16° , 47.86° , and 70.17° 2θ , which are assigned to the crystal planes of (111), (220), and (220), respectively. According to the reference of (JCPDS 05-0685), these peaks are in the exact locations of metallic rhodium (Rh^0) particles [32]. Moreover, these peaks were found to be developed with the Rh content, which is in a good agreement with the elemental analysis. The change from Rh_2O_3 to Rh^0 can be attributed to the total reduction after the hydrogenation step and the formation of the desired metallic active sites. Finally, no other crystalline phase could be observed, as an indication of the high purity of the prepared samples.

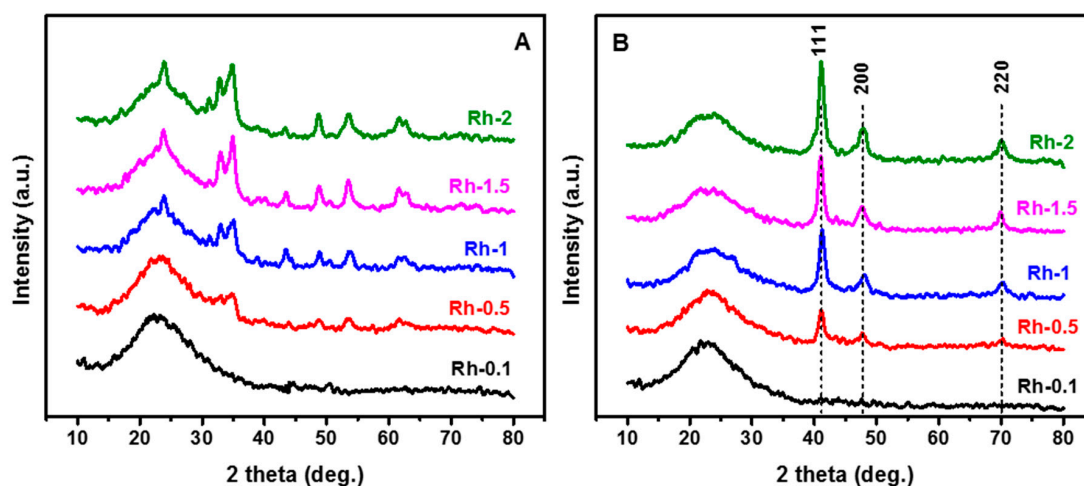


Figure 2. XRD patterns of the prepared Rh-TUD-1 samples: (A) The as-synthesized samples, and (B) the hydrogenated samples and the formation of the final products.

The morphology of the samples was investigated by SEM. The micrograph of the Rh-1 sample is presented in Figure 3 (left panel). The obtained micrographs showed that the particles of Rh-TUD-1 have an irregular shape, which is characteristic of the TUD-1 mesoporous material [33]. No other foreign bulky crystals could be observed, as an indication of the presence of Rh particles inside/outside the particles in nanosize, and no crystals of Rh are formed outside the framework. Moreover, an EDX analysis (Figure 3, right panel) showed only the peaks of the Si, O, and Rh elements. No other metals were determined, as an indication of the high purity of the prepared samples, which is in agreement with the obtained XRD results.

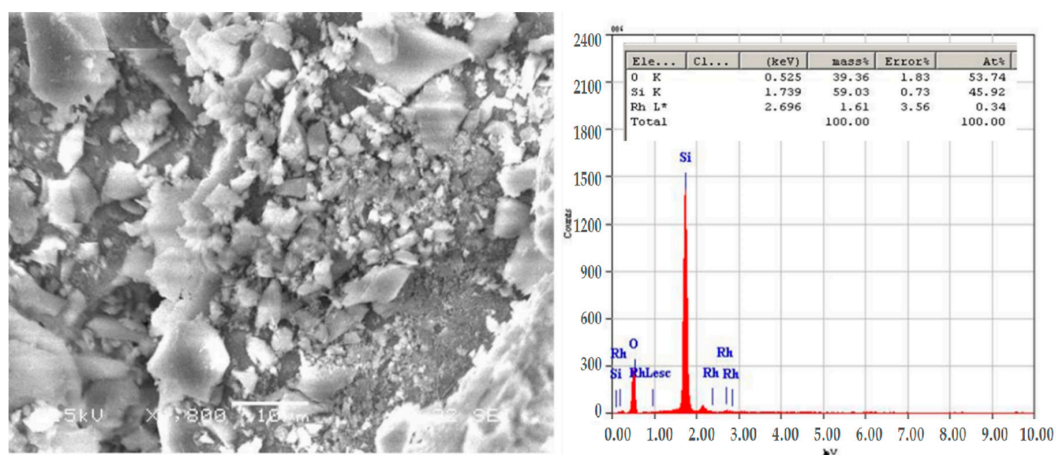


Figure 3. Left panel: The SEM micrograph of the Rh-1 sample. Right panel: the corresponding EDX analysis, inset: the elemental analysis as obtained from EDX

The distribution of the Rh nanoparticles inside the silica matrix was studied using HR-TEM. The micrographs of the Rh-1 sample (Figure 4) showed a high distribution of Rh nanoparticles. Moreover, the size of the nanoparticles was estimated to be 3–5 nm for all the prepared samples.

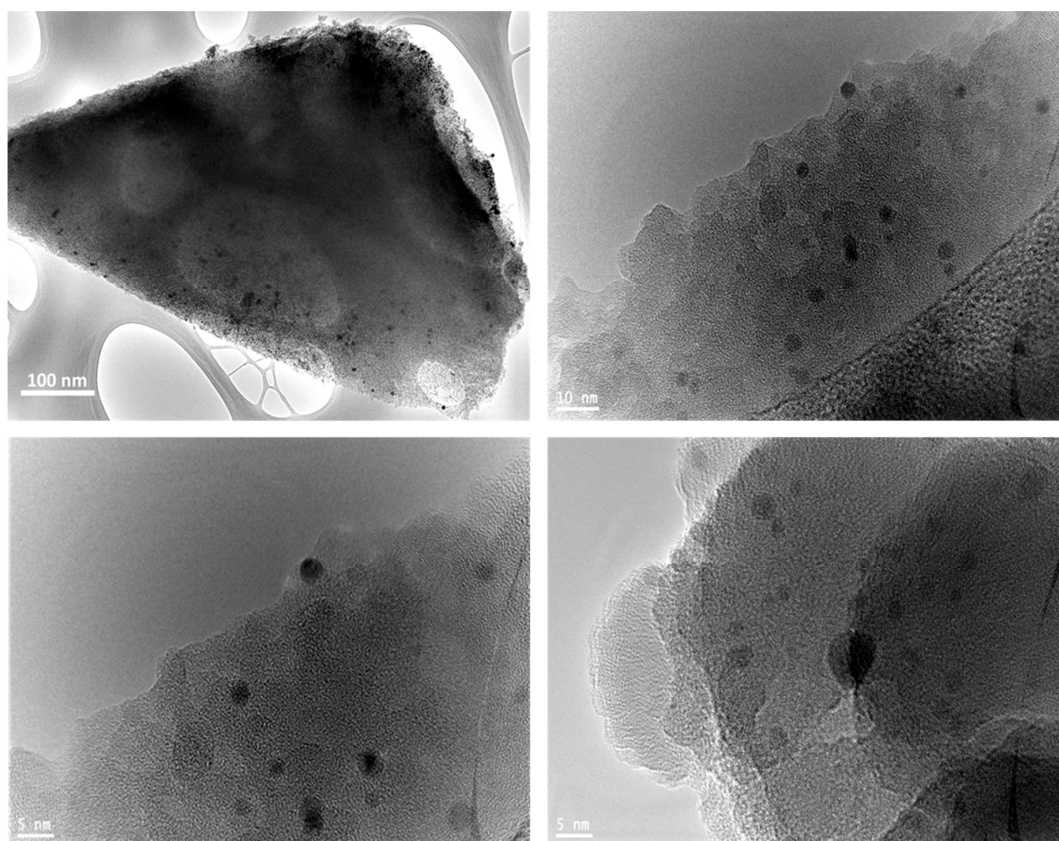


Figure 4. HR-TEM micrographs of the Rh-1 sample.

The chemical state of the surface elements in addition to the chemical composition of the catalysts were investigated using the XPS technique. The obtained results are presented in Figure 5. For all the samples, the two peaks, which were located at values of about 103.85 and 533.01 eV, were attributed to Si2p and O1s, respectively, according to previous reports [34,35]. The XPS profile of Rh-TUD-1 shows

the binding energies of Rh 3d_{5/2} and Rh 3d_{3/2} around 307.6 eV and 311.8 eV, respectively, which can be assigned to the presence of Rh⁰ as a metallic nanoparticle on the mesoporous surface of Rh-TUD-1 catalyst [36,37]. Besides, the XPS analysis showed also the presence of some surface carbon at 283.6 eV, which can be related to the incomplete removal of the template during the calcination step.

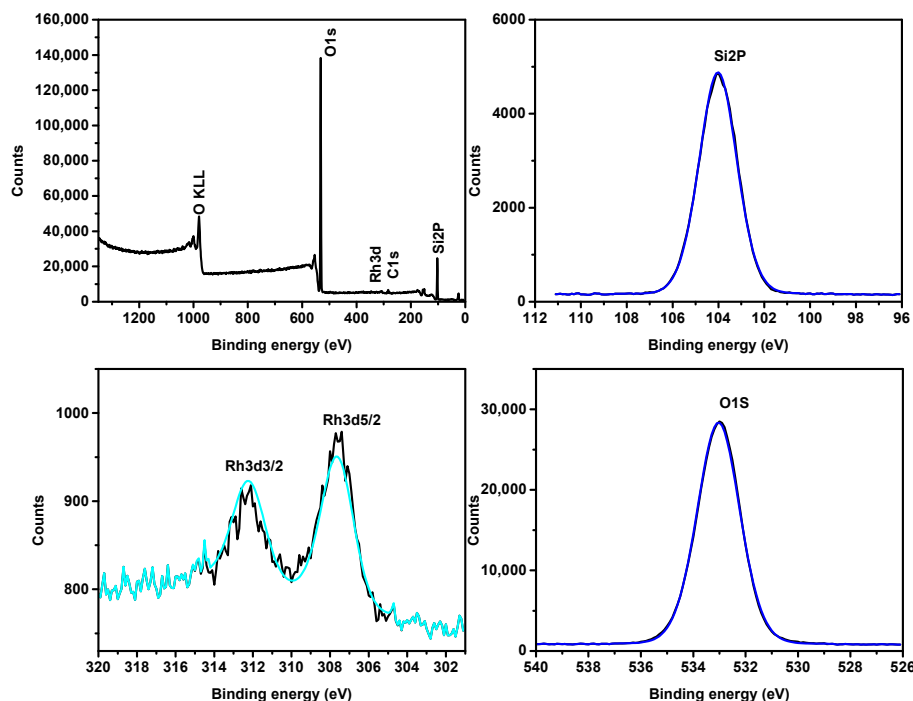


Figure 5. XPS analysis for the Rh-1 sample.

2.2. The Catalytic Activity of the Prepared Catalysts

The catalytic performance of the Rh-TUD-1 sample was investigated in the hydrogenation of cyclohexene to produce cyclohexane as a solo product. The reaction was performed under solvent-free ambient conditions, room temperature, and 1 atm H₂ pressure. The obtained conversion as a function of the reaction time is plotted in Figure 6a. After 120 min, the Rh-2 sample catalyzed the conversion of almost the entire amount of cyclohexene; the Rh-1.5 sample catalyzed the conversion of 91.3%; while Rh-1, Rh-0.5, and Rh-0.1 catalyzed the conversion of 78.9%, 47.9%, and 32.3%, respectively. The obtained results showed a clear trend that cyclohexene conversion is increased by increasing the Rh content without limitation up to 2 wt%.

The calculated TOF after one hour is presented with the corresponding conversion % in Figure 6b. The results showed that the Rh-0.1 sample exhibited the highest TOF, in which 4.94 micromoles of cyclohexene were converted over one micromole of Rh active phase per second. Moreover, Rh-0.5 and -1 showed a TOF of 1.43 and 0.91 s⁻¹, respectively. Finally, a small difference was obtained between the Rh-1.5 and Rh-2 samples, where TOF values of 0.69 and 0.54 s⁻¹ were obtained, respectively. This result can be attributed to the high distribution of Rh nanoparticles inside the TUD-1 sample for the low loading samples, which gives a high surface area of the Rh nanoparticles in addition to easy access to/from the Rh⁰ active sites.

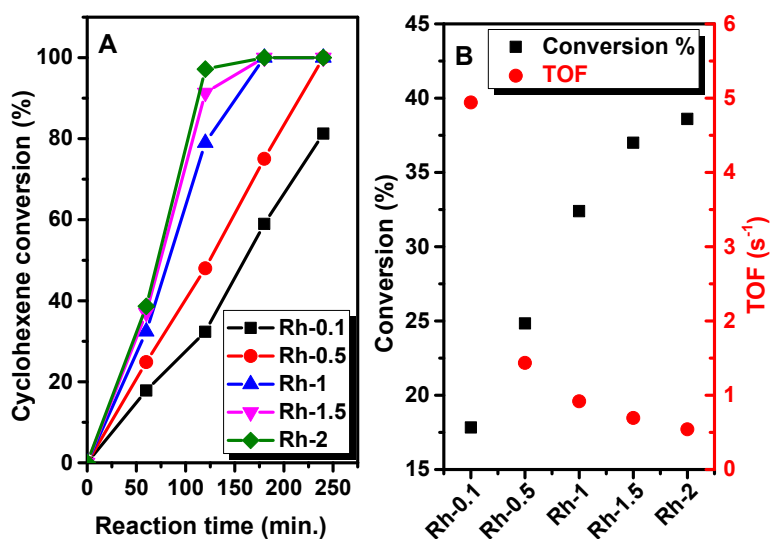


Figure 6. (A) The conversion profiles of cyclohexene reduction over different Rh-TUD-1 samples within 4 h of reaction. (B) The obtained conversion of cyclohexene and the corresponding TOF (s⁻¹) after 1 h of reaction.

The change in the reactor's temperature during the hydrogenation of cyclohexene over different Rh-TUD-1 samples was monitored. The obtained results are introduced in Figure 7, and show an obvious increase in the reactor's temperature as a function of the reaction time. The reported increase in the reactor's temperature is increased with the Rh content in the prepared samples. This result clearly indicates that the hydrogenation of cyclohexene over Rh-TUD-1 is a spontaneous reaction with an exothermic nature.

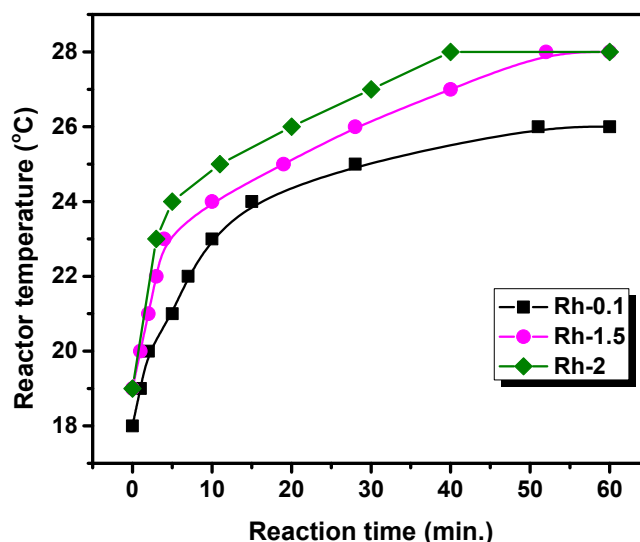


Figure 7. The change in the reactor's temperature during the hydrogenation of cyclohexene over Rh-TUD-1 samples as a function of the reaction time.

In order to optimize the ratio of substrate/catalyst, the reactions were performed with different amount of the Rh-TUD-1 samples, 0.1, 0.25, and 0.4 g for each 25 mL of cyclohexene. The reactions were performed for one hour and the obtained results are plotted in Figure 8. The obtained data showed that the conversion of cyclohexene was increased as the amount of catalyst increased, which is valid for the investigated samples. The increase in the cyclohexene conversion % was not linearly proportional

to the catalyst amount; this can be attributed to the mass transfer limitation which occurred due to the increase in the catalyst amount.

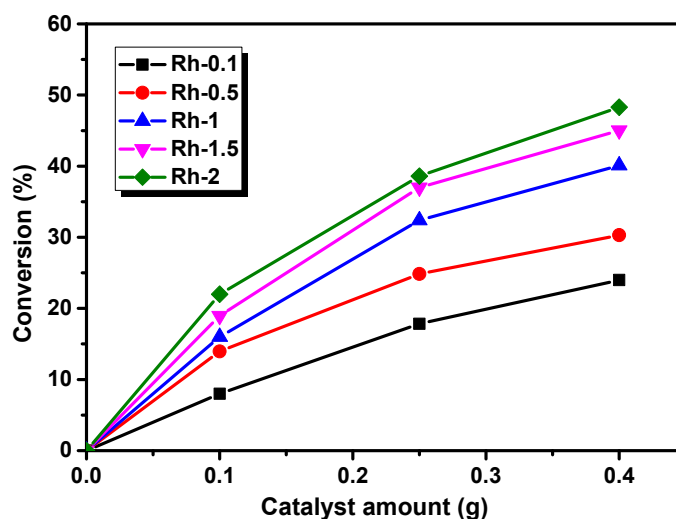


Figure 8. The cyclohexene conversion % as a function of the catalyst amount for 1 s reaction.

The above-mentioned results were entirely obtained under ambient conditions and without the use of any solvent. In order to investigate the catalytic behavior of Rh-TUD-1 samples under non-ambient conditions, the hydrogenation of cyclohexene reactions were performed at 60 °C and 5 atm of H₂ gas pressure. The reactions were performed for only one hour, and the obtained results are compared with those of the reactions which were performed under ambient conditions in Figure 9a. The obtained results showed that the Rh-0.1 sample was able to convert 82.3% under the non-ambient conditions, which is almost four times higher than its activity under the ambient conditions. The rest of the Rh-TUD-1 samples exhibited a 100% cyclohexene conversion with a high TOF (s⁻¹), as shown in Figure 9b.

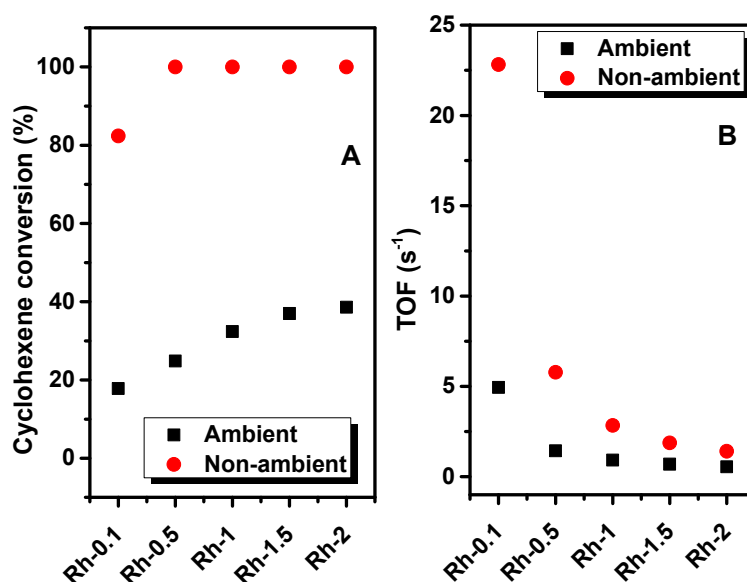


Figure 9. (A) A comparison between the catalytic activity of the Rh-TUD-1 under ambient and non-ambient conditions. (B) The corresponding TOF (s⁻¹).

The stability of the Rh-2 sample was investigated under ambient and non-ambient conditions in which the same sample of the catalyst was allowed to catalyze five consecutive reactions of cyclohexene

hydrogenation. The obtained results are plotted in Figure 10, and showed that the Rh-2 sample was stable and only a negligible amount of deactivation (<3.5%) could be observed after the fifth run. Moreover, a leaching study was performed by investigating the amount of Rh either in the dried solid used catalyst or in the reaction medium using an ICP elemental analysis. Rh nanoparticles were stable inside the pores of TUD-1, and less than 4% of the total Rh content was lost after the fifth run.

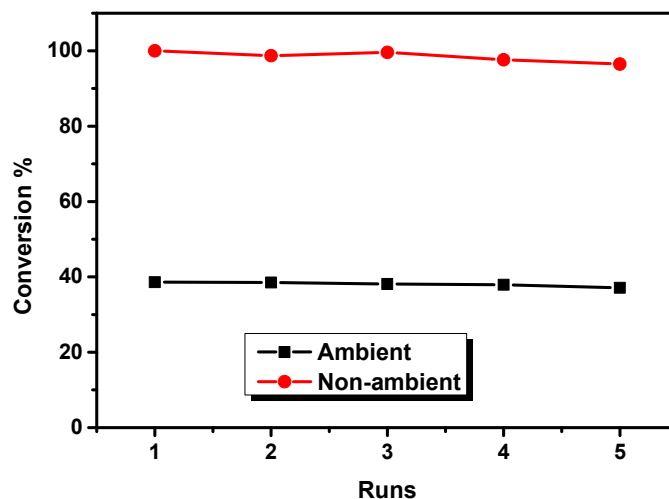


Figure 10. The activity of the Rh-2 sample in five consecutive runs of cyclohexene hydrogenation under ambient and non-ambient conditions.

3. Discussion

As shown from the obtained characterization results, the use of TUD-1 to accommodate Rh nanoparticles has several advantages, which will be presented in this section. The synthesis of Rh-TUD-1 was performed in a one-step sol-gel procedure using the small-molecule triethanol amine as a template; copolymer(s) and/or long-chain surfactant(s) were not needed to achieve the desired structure. TUD-1 accommodated Rh nanoparticles at up to 2 wt% without an aggregation in the Rh nanoparticles, which reflects the catalytic behavior of the prepared Rh-TUD-1 sample. Moreover, the three-dimensional open structure of TUD-1 offered high accessibility to the substrates in order to reach/leave the active sites, and no mass-transfer limitation was observed. Similar results of the importance of TUD-1 as compared to other mesoporous materials were discussed in [38–40]. Moreover, it is believed that the majority of Rh nanoparticles are located inside the mesopores of TUD-1, and therefore Rh-TUD-1 exhibited a high stability even under 1000 rpm of mechanical stirring with a pressure of 5 atm of hydrogen gas.

From the obtained results, it is clearly seen that Rh-TUD-1 exhibited a high activity in the liquid-phase hydrogenation of cyclohexene under ambient conditions and without the use of any solvent. For comparison purposes, four other noble metals (with 1 wt% loading, each) incorporating TUD-1 mesoporous material were tested under the same reaction conditions; the obtained results are plotted in Figure 11. Gold and silver nanoparticles incorporating TUD-1 did not show any catalytic activity in cyclohexene hydrogenation. On the other hand, platinum nanoparticles exhibited a 3.2% conversion, while palladium was able to convert 16.2% of the cyclohexene under ambient conditions. Rh-TUD-1 exhibited the highest activity, and it was able to catalyze the conversion of 32.3% of the cyclohexene. These results showed clearly that the combination of Rh nanoparticles as active sites and TUD-1 as a support for these nanoparticles produced an active, stable, and promising catalyst for the hydrogenation of cyclohexene.

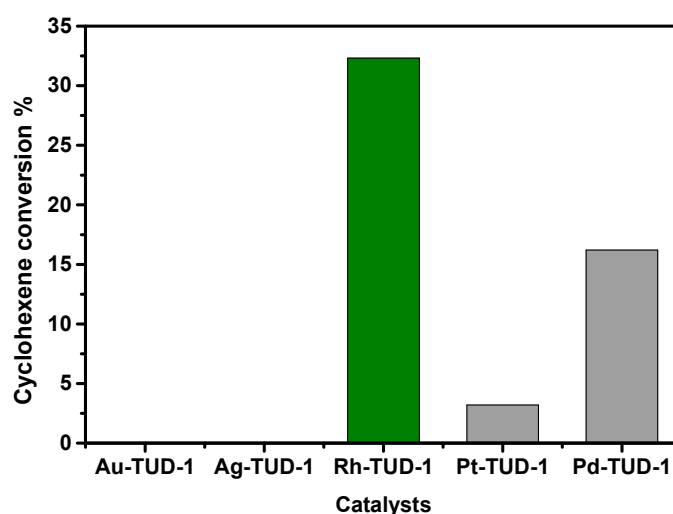


Figure 11. Comparison between the activity of different noble metals incorporating TUD-1 in the hydrogenation of cyclohexene under solvent-less and ambient conditions.

In order to evaluate the obtained catalytic activity during the current study with the other homogeneous and heterogeneous catalysts, a comparison with the published Rh-based catalysts was performed. Table 2 lists a comparison of the TOFs (s^{-1}) obtained by different catalytic systems. The results of the Rh-0.1 sample were chosen for this comparison because it contained the smallest Rh loading amongst all the Rh-TUD-1 samples. It is obviously clear that the Rh-0.1 sample exhibited the best performance either under ambient conditions or under elevated temperature and/or pressure.

Table 2. A comparison between the catalytic activity expressed in the turnover frequency (TOF, s^{-1}) of the Rh-TUD-1 catalyst and other reported Rh-based homogeneous or heterogeneous catalysts.

Catalyst	Type	Reaction Conditions	TOF (s^{-1})	Ref.
T20-RhCOD	Homogeneous	Solvent (toluene), 60 °C, 10 bar H_2	0.094	[16]
RhPVP	Homogeneous	Solvent-free, 75 °C, 6 bar of H_2	0.972	[17]
RhPPh ₃	Homogeneous	Solvent-free, 75 °C, 6 bar of H_2	1.05	[17]
Rh-Au core shell	heterogeneous	Gas phase, room T	≈7	[19]
Rh/SiO ₂	heterogeneous	Gas phase, room T, 14 KPa H_2	1.7	[41]
Rh-0.1	heterogeneous	Solvent-free, room T, 1 atm H_2	4.94	current
Rh-0.1	heterogeneous	Solvent-free, 60 °C, 5 atm H_2	22.8	current

The obtained results and the comparison with other catalysts clearly show that the Rh-TUD-1 catalyst benchmarked not only the noble metals incorporating TUD-1 but also other reported homogeneous or heterogeneous catalysts. It is also important that such a high activity was obtained at room temperature and at 1atm of H_2 gas; moreover, no solvent is needed for cyclohexene, and this adds another advantage to the use of Rh-TUD-1 in hydrogenation reactions.

Over the nanoparticles of Rh^0 , the hydrogenation reaction can proceed in three main steps: 1—Adsorption: The hydrogen molecules are adsorbed on the Rh nanoparticles, followed by fast dissociation to form an H-Rh bond. Moreover, the cyclohexene molecules are adsorbed also on the Rh surface and the double bond cleaves. 2—Reaction: One H will attach to one side of the ex-double bonded carbon. Then, the second hydrogen atom is added to the second carbon of the ex-double bond to form the cyclohexane product. 3—Desorption: the formed cyclohexane is desorbed from the Rh surface and then the surface is clean to start a new reaction. Figure 12 shows a schematic diagram for the steps of the reaction mechanism.

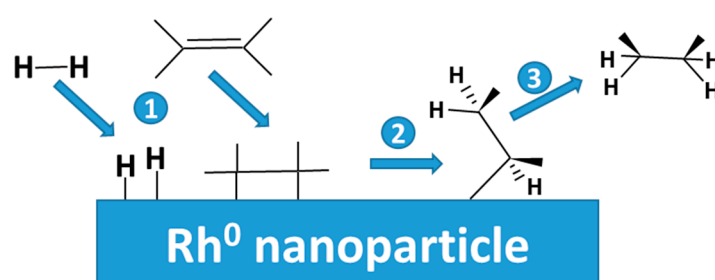


Figure 12. The proposed mechanism for the hydrogenation of cyclohexene over Rh-TUD-1.

4. Materials and Methods

Five samples consist of Rh nanoparticles incorporating TUD-1 mesoporous material with different Rh loadings. The Rh content in the samples was 0.1, 0.5, 1.0, 1.5, and 2 wt%. The applied synthesis procedure was based on the sol-gel technique using triethanol amine as a small-size template. The exact synthesis procedure was adapted by the method developed by Hamdy et al. in [12,16]. In the exact synthesis procedure, a solution of rhodium (III) nitrate hydrate ($\text{Rh}(\text{NO}_3)_3 \cdot x\text{H}_2\text{O}$, Sigma-Aldrich) was mixed with a dilute solution of triethanol amine (TEA, 97%, ACROS). The resultant solution was added dropwise to tetraethyl orthosilicate (TEOS, +98%, ACROS) under vigorous stirring at room temperature. The resulting homogeneous solution/gel was aged at room temperature for 24 h, and then dried at 98 °C for another 24 h. The obtained solid was grinded and thermally treated in a 50 mL Teflon-lined stainless-steel autoclave at 178 °C under autogenous pressure for 4 h. The obtained solid was carefully ground, and then calcined in static air at 600 °C for 10 h by applying a heating ramp rate of 1 degree/min. The synthesis was applied by using the composition ratio of $10\text{SiO}_2 : x\text{Rh} : 5\text{TEAOH} : 10\text{TEA} : 200\text{H}_2\text{O}$ (where $0.01 < x < 0.2$). Finally, the prepared RH-TUD-1 samples were hydrogenated in a tube furnace at 300 °C for 3 h to ensure the reduction of the as-synthesized RhO to Rh⁰ nanoparticles in the final products. The obtained materials were stored in clean glass vials and coded as Rh-x, where x is the Rh content as calculated before the synthesis.

The Rh content in the prepared samples before and after the reactions was performed using the inductive coupled plasma (ICP) technique over Thermo scientific (Waltham, MA, USA), ICAP 7000 series, part No: 1340910, Qtegra Software (1.3.882.20) (Waltham, MA, USA). Calibration curves were performed first using standard solutions of rhodium nitrate. The texture properties of the prepared samples were calculated from the nitrogen adsorption/desorption measurements. The N₂ sorption isotherms were collected using a QuantaChrome NOVA 2000e instrument (Quantachrome Instruments, Boynton Beach, FL, USA). The investigated samples were degassed at 300 °C for four hours to ensure the removal of any volatile residuals from the internal or external surfaces of the catalysts. The Brunauer–Emmett–Teller (BET) model was used to calculate the total surface area of the samples. Meanwhile, the pore size distribution was calculated from the adsorption branch using the Barret–Joyner–Halenda (BJH) model, and the t-plot method was applied to calculate the mesopore volume. The degree of crystallinity and phase identification was investigated by powder X-ray diffraction (XRD) using a Shimadzu 6000 DX instrument diffractometer (Shimadzu Corporation, Kyoto, Japan) equipped with a graphite monochromator using CuK radiation ($\lambda = 0.1541 \text{ nm}$). The samples were carefully ground, held in an aluminum holder, and screened from 10° to 80° 2 θ . The morphology of the samples was investigated by scanning electron microscopy (SEM), which was carried out using Jeol Model 6360LVSEM (JEOL Inc., Peabody, MA, USA). The investigated samples were coated first with gold, and then micrographs with different magnifications were obtained. Using the X-ray spectroscopy (EDX) unit which was equipped in the SEM instrument, a semi-quantitative elemental analysis was performed. The size and distribution of the Rh nanoparticles were observed using high-resolution transmission electron microscopy (HR-TEM). The study was carried out using a Philips CM30UT electron microscope (Philips Electronics, Eindhoven, The Netherlands) with a field

emission gun as the source of electrons, and was operated at 300 kV. The investigated materials were mounted on a copper-supported carbon polymer grid by placing a few droplets of a suspension of the ground sample in ethanol on the grid, followed by drying in ambient conditions. The oxidation state of the different species was investigated by X-ray photoelectron spectroscopy (XPS). The applied instrument was PHI 5400 ESCA (ULVAC-PHI, Inc., Kanagawa, Japan), equipped with a dual Mg/Al anode X-ray source, a hemispherical capacitor analyzer, and a 5 keV ion gun. A survey spectrum was recorded between a 0 and 1350 eV binding energy, using a pass energy of 71.95 eV and a step size of 0.3 eV. The spectra of the separate photoelectron or Auger electron lines were recorded with a pass energy of 35.75 eV and a step size of 0.2 eV. All the measurements were carried out at room temperature.

The catalytic activity of the prepared samples was investigated in the reduction of cyclohexene using hydrogen gas as a reducing agent. The reduction of cyclohexene was performed under solvent-free conditions in ambient conditions—i.e., room temperature and 1 atm of H₂ gas—in a stirred batch Parr reactor with a 300 mL capacity. In an exact experiment, 0.25 g of the carefully ground catalyst was placed inside the reactor with 25 mL of cyclohexene ($\geq 99\%$, Sigma-Aldrich). The autoclave was closed and flushed twice with nitrogen (15 mg/L for 15 min each) and finally pressurized to the necessary pressure with hydrogen gas. Then, the reaction was vigorously stirred (up to 1000 rpm) to minimize the external mass transfer limitations. After the reaction time elapsed, the reactor was flushed with nitrogen and then a liquid sample was withdrawn and filtrated. The concentrations of cyclohexene and cyclohexane (the product) were analyzed using a SHIMADZU GC-17 instrument equipped with an RTX-5 capillary column (30 m \times 0.25 mm \times 0.25 μ m) and a flame ionization detector (FID). All the experiments were performed at least three times, the experimental error did not exceed $\pm 4\%$, and the reported data is the average of the three experiments. The conversion of cyclohexene (CXE) was calculated according to the following equation:

$$\text{Conversion\%} = \frac{[\text{CXE}]_0 - [\text{CXE}]_t}{[\text{CXE}]_0} \times 100,$$

where $[\text{CXE}]_0$ is the initial concentration of cyclohexene, $[\text{CXE}]_t$ is the concentration of cyclohexene at time (t). On the other hand, the turnover frequency (TOF) was calculated according to the equation:

$$\text{TOF} \left(\text{s}^{-1} \right) = \frac{\text{Reacted moles of CXE}}{\text{Moles of Rh} \times \text{time(s)}}.$$

5. Conclusions

Rh nanoparticles with an average size between 3 and 5 nm were incorporated successfully in TUD-1 mesoporous silica material in a one-step synthesis. The prepared samples exhibited high activity in the hydrogenation of cyclohexene to cyclohexane under ambient conditions and without any solvent. The catalytic activity was found to be increased with the Rh loading, and 100% conversion was obtained within one hour of reaction. Moreover, controlling the temperature of the reactor gave an indication of the nature of the reaction, which is a spontaneous and exothermic reaction. Rh-TUD-1 exhibited a good activity, and the catalysts were stable for five consecutive runs, even under elevated temperature and pressure. The activity of Rh-TUD-1 benchmarked that of other noble metals incorporating TUD-1 mesoporous material such as gold, silver, platinum, and palladium.

Author Contributions: Conceptualization, M.S.H. and A.M.A.; methodology, M.S.H. and M.B.; characterization, A.A., F.A.A., and N.A.-Z.; writing—original draft preparation, M.S.H. and A.M.A. All the authors have read and agreed to the published version of the manuscript.

Funding: This research was funded by Deanship of Scientific Research at King Khalid University, grant number R.G.P1/115/40, and the characterizations were funded by Deanship of Scientific Research at King Saud University, grant number RG-1440-141.

Acknowledgments: The authors sincerely acknowledge the Deanship of Scientific Research at King Khalid University for funding this work through a research group project number R.G.P1/115/40. Moreover, the authors extend also their appreciation to the Deanship of Scientific Research at King Saud University for funding this work through research group no. (RG-1440-141).

Conflicts of Interest: The authors declare no conflict of interest.

References

1. David Jackson, S. *Hydrogenation: Catalysts and Processes*; De Gruyter: Berlin, Germany, 2018. [[CrossRef](#)]
2. Seo, C.S.; Morris, R.H. Catalytic homogeneous asymmetric hydrogenation: Successes and opportunities. *Organometallics* **2018**, *38*, 47–65. [[CrossRef](#)]
3. Yang, M.; Rioux, R.M.; Somorjai, G.A. Reaction kinetics and in situ sum frequency generation surface vibrational spectroscopy studies of cycloalkene hydrogenation/dehydrogenation on Pt (111): Substituent effects and CO poisoning. *J. Catal.* **2006**, *237*, 255–266. [[CrossRef](#)]
4. Jackson, S.D.; Kelly, G.J.; Watson, S.R.; Gulickx, R. Cycloalkene hydrogenation over palladium catalysts. *Appl. Catal. A* **1999**, *187*, 161–168. [[CrossRef](#)]
5. Hereijgers, B.P.; Weckhuysen, B.M. Aerobic oxidation of cyclohexane by gold-based catalysts: New mechanistic insight by thorough product analysis. *J. Catal.* **2010**, *270*, 16–25. [[CrossRef](#)]
6. Schuchardt, U.; Cardoso, D.; Sercheli, R.; Pereira, R.; Da Cruz, R.S.; Guerreiro, M.C.; Mandelli, D.; Spinacé, E.V.; Pires, E.L. Cyclohexane oxidation continues to be a challenge. *Appl. Catal. A* **2001**, *211*, 1–17. [[CrossRef](#)]
7. Schumacher, C.; Crawford, D.E.; Raguž, B.; Glaum, R.; James, S.L.; Bolm, C.; Hernández, J.G. Mechanochemical dehydrocoupling of dimethylamine borane and hydrogenation reactions using Wilkinson’s catalyst. *Chem. Commun.* **2018**, *54*, 8355–8358. [[CrossRef](#)]
8. Augustine, R.L.; Yaghmaie, F.; Van Peppen, J.F. Heterogeneous catalysis in organic chemistry. 2. A mechanistic comparison of noble-metal catalysts in olefin hydrogenation. *J. Org. Chem.* **1984**, *49*, 1865–1870. [[CrossRef](#)]
9. Gong, L.H.; Cai, Y.Y.; Li, X.H.; Zhang, Y.N.; Su, J.; Chen, J.S. Room-temperature transfer hydrogenation and fast separation of unsaturated compounds over heterogeneous catalysts in an aqueous solution of formic acid. *Green Chem.* **2014**, *16*, 3746–3751. [[CrossRef](#)]
10. Mao, H.; Peng, S.; Yu, H.; Chen, J.; Zhao, S.; Huo, F. Facile synthesis of highly stable heterogeneous catalysts by entrapping metal nanoparticles within mesoporous carbon. *J. Mater. Chem. A* **2014**, *16*, 5847–5851. [[CrossRef](#)]
11. Humbert, M.P.; Chen, J.G. Correlating hydrogenation activity with binding energies of hydrogen and cyclohexene on M/Pt (111)(M= Fe, Co, Ni, Cu) bimetallic surfaces. *J. Catal.* **2008**, *257*, 297–306. [[CrossRef](#)]
12. Oliveira, D.G.; Rosa, G.R.; Scheeren, C.W. Rh and Pd Nanoparticles Supported in a Polymeric Membrane: Evaluation in Hydrogenation and Suzuki-Miyaura Reactions. *J. Nanosci. Nanotechnol.* **2017**, *17*, 9295–9301. [[CrossRef](#)]
13. Ghadamgahi, S.; Johnston, J.H.; Fonseca-Paris, C. Ecofriendly Palladium on Wool Nanocatalysts for Cyclohexene Hydrogenation. *Nanomaterials* **2018**, *8*, 621. [[CrossRef](#)] [[PubMed](#)]
14. Eberhardt, D.; Migowski, P.; Teixeira, S.R.; Feil, A.F. Templated Growth of Pd Nanoparticles Using Sputtering Deposition Process and Its Catalytic Activities. *J. Nanosci. Nanotechnol.* **2018**, *18*, 2075–2078. [[CrossRef](#)] [[PubMed](#)]
15. Patel, A.; Patel, A.; Narkhede, N. Hydrogenation of Cyclohexene in Aqueous Solvent Mixture Over a Sustainable Recyclable Catalyst Comprising Palladium and Monolacunary Silicotungstate Anchored to MCM-41. *Eur. J. Inorg. Chem.* **2019**, *2019*, 423–429. [[CrossRef](#)]
16. Rufete-Beneite, M.; Román-Martínez, M.C. Unraveling Toluene Conversion during the Liquid Phase Hydrogenation of Cyclohexene (in Toluene) with Rh Hybrid Catalysts. *Catalysts* **2019**, *9*, 973. [[CrossRef](#)]
17. Ibrahim, M.; Garcia, M.A.; Vono, L.L.; Guerrero, M.; Lecante, P.; Rossi, L.M.; Philippot, K. Polymer versus phosphine stabilized Rh nanoparticles as components of supported catalysts: Implication in the hydrogenation of cyclohexene model molecule. *Dalton Transact.* **2016**, *45*, 17782–17791. [[CrossRef](#)] [[PubMed](#)]
18. Dahal, N.; Garcia, S.; Zhou, J.; Humphrey, S.M. Beneficial effects of microwave-assisted heating versus conventional heating in noble metal nanoparticle synthesis. *ACS Nano* **2012**, *6*, 9433–9446. [[CrossRef](#)]

19. García, S.; Anderson, R.M.; Celio, H.; Dahal, N.; Dolocan, A.; Zhou, J.; Humphrey, S.M. Microwave synthesis of Au–Rh core–shell nanoparticles and implications of the shell thickness in hydrogenation catalysis. *Chem. Commun.* **2013**, *49*, 4241–4243. [[CrossRef](#)]
20. Benaissa, M.; Alhanash, A.M.; Mubarak, A.T.; Eissa, M.; Sahlabji, T.; Hamdy, M.S. Solvent-free hydrogenation of cyclohexene over Rh-TUD-1 at ambient conditions. *RSC Adv.* **2018**, *8*, 34370–34373. [[CrossRef](#)]
21. Benaissa, M.; Alhanash, A.M.; Eissa, M.; Hamdy, M.S. Solvent-free selective hydrogenation of 1,5-cyclooctadiene catalyzed by palladium incorporated TUD-1. *Catal. Commun.* **2017**, *101*, 62–65. [[CrossRef](#)]
22. Mubarak, A.T.; Alhanash, A.M.; Benaissa, M.; Hegazy, H.H.; Hamdy, M.S. In-situ activation of Pd-TUD-1 during the selective reduction of 1,5-cyclooctadiene. *Microporous Mesoporous Mater.* **2019**, *278*, 225–231. [[CrossRef](#)]
23. Jansen, J.C.; Shan, Z.; Marchese, L.; Zhou, W.; vd Puil, N.; Maschmeyer, T. A new templating method for three-dimensional mesopore networks. *Chem. Commun.* **2001**, *8*, 713–714. [[CrossRef](#)]
24. Hamdy, M.S. Au-TUD-1: A new catalyst for aerobic oxidation of cyclohexene. *Microporous Mesoporous Mater.* **2016**, *220*, 81–87. [[CrossRef](#)]
25. Hamdy, M.S.; Mul, G. Synthesis, characterization and catalytic performance of Mo-TUD-1 catalysts in epoxidation of cyclohexene. *Catal. Sci. Technol.* **2012**, *2*, 1894–1900. [[CrossRef](#)]
26. Hamdy, M.S.; Mul, G. The effect of active sites' nature on the photo-catalytic performance of Cr-TUD-1 in the oxidation of C1–C3 hydrocarbons. *Appl. Catal. B* **2015**, *174*, 413–420. [[CrossRef](#)]
27. Mul, G.; Wasylenko, W.; Hamdy, M.S.; Frei, H. Cyclohexene photo-oxidation over vanadia catalyst analyzed by time resolved ATR-FT-IR spectroscopy. *Phys. Chem. Chem. Phys.* **2008**, *10*, 3131–3137. [[CrossRef](#)]
28. Hamdy, M.S.; Eissa, M.A.; Keshk, S.M. New catalyst with multiple active sites for selective hydrogenolysis of cellulose to ethylene glycol. *Green Chem.* **2017**, *19*, 5144–5151. [[CrossRef](#)]
29. Sing, K.S. Reporting physisorption data for gas/solid systems with special reference to the determination of surface area and porosity (Recommendations 1984). *Pure Appl. Chem.* **1985**, *57*, 603–619. [[CrossRef](#)]
30. Hamdy, M.S.; Mul, G.; Jansen, J.C.; Ebaid, A.; Shan, Z.; Overweg, A.R.; Maschmeyer, T. Synthesis, characterization, and unique catalytic performance of the mesoporous material Fe-TUD-1 in Friedel–Crafts benzylolation of benzene. *Catal. Today* **2005**, *100*, 255–260. [[CrossRef](#)]
31. Park, J.C. Purification and recovery of rhodium metal by the formation of intermetallic compounds. *Bull. Korean Chem. Soc.* **2008**, *29*, 1787–1789.
32. Chen, H.; Lu, Q.; Yi, C.; Yang, B.; Qi, S. Bimetallic Rh–Fe catalysts for N₂O decomposition: Effects of surface structures on catalytic activity. *Phys. Chem. Chem. Phys.* **2018**, *20*, 5103–5111. [[CrossRef](#)] [[PubMed](#)]
33. Lima, S.; Antunes, M.M.; Fernandes, A.; Pillinger, M.; Ribeiro, M.F.; Valente, A.A. Acid-catalysed conversion of saccharides into furanic aldehydes in the presence of three-dimensional mesoporous Al-TUD-1. *Molecules* **2010**, *15*, 3863–3877. [[CrossRef](#)] [[PubMed](#)]
34. Grunthaner, F.J.; Grunthaner, P.J.; Vasquez, R.P.; Lewis, B.; Maserjian, J.; Madhukar, A. Local atomic and electronic structure of oxide/GaAs and SiO₂/Si interfaces using high-resolution XPS. *J. Vac. Sci. Technol.* **1979**, *16*, 1443–1453. [[CrossRef](#)]
35. López, G.P.; Castner, D.G.; Ratner, B.D. XPS O1s binding energies for polymers containing hydroxyl, ether, ketone and ester groups. *Surf. Interface Anal.* **1991**, *17*, 267–272. [[CrossRef](#)]
36. Su, P.; Chen, Y.; Liu, X.; Chuai, H.; Liu, H.; Zhu, B.; Huang, W. Preparation and Characterization of Rh/MgSNTs Catalyst for Hydroformylation of Vinyl Acetate: The Rh⁰ was obtained by calcination. *Catalysts* **2019**, *9*, 215. [[CrossRef](#)]
37. Simagina, V.I.; Storozhenko, P.A.; Netskina, O.V.; Komova, O.V.; Odegova, G.V.; Larichev, Y.V.; Ishchenko, A.V.; Ozerova, A.M. Development of catalysts for hydrogen generation from hydride compounds. *Catal. Today* **2008**, *138*, 253–259. [[CrossRef](#)]
38. Guo, Z.; Zhou, C.; Hu, S.; Chen, Y.; Jia, X.; Lau, R.; Yang, Y. Epoxidation of trans-stilbene and cis-cyclooctene over mesoporous vanadium catalysts: Support composition and pore structure effect. *Appl. Catal. A* **2012**, *419*, 194–202. [[CrossRef](#)]
39. Pachamuthu, M.P.; Srinivasan, V.V.; Maheswari, R.; Shanthi, K.; Ramanathan, A. The impact of the copper source on the synthesis of meso-structured CuTUD-1: A promising catalyst for phenol hydroxylation. *Catal. Sci. Technol.* **2013**, *3*, 3335–3342. [[CrossRef](#)]

40. Wang, X.; Song, C.; Gaffney, A.M.; Song, R. New molecular basket sorbents for CO₂ capture based on mesoporous sponge-like TUD-1. *Catal. Today* **2014**, *238*, 95–102. [[CrossRef](#)]
41. Da Cruz, G.M.; Bugli, G.; Djega-Mariadassou, G. Cyclohexene hydrogenation on rhodium catalysts in the gas phase: Kinetics of the reaction and origin, mechanism and kinetics of the deactivation process: Kinetics of the reaction and origin, mechanism and kinetics of the deactivation process. *Appl. Catal.* **1989**, *46*, 131–144. [[CrossRef](#)]



© 2020 by the authors. Licensee MDPI, Basel, Switzerland. This article is an open access article distributed under the terms and conditions of the Creative Commons Attribution (CC BY) license (<http://creativecommons.org/licenses/by/4.0/>).